COMPARATIVE ANALYSIS OF TWO DIFFERENT NITI WIRES' PROPERTIES AND FATIGUE LIFE*

Lorena Isabela de Oliveira Ribeiro[1]
João Victor Lucas Amim[2]
Pedro Damas Resende[3]
Jéssica Dornelas Silva[4]
Suzanny Cristina Soares Martins[5]
Leandro de Arruda Santos[6]
Vicente Tadeu Lopes Buono[7]

Resumo

O objetivo do presente estudo foi avaliar a resistência à fadiga de duas ligas de NiTi diferentes sob condições de teste controladas por deformação a 25°C por meio de testes de fadiga por flexão rotativa. Além disso, as propriedades mecânicas, térmicas e estruturais dos fios foram caracterizadas por ensaios de DSC, DRX, MEV/EDS e tração. Os resultados revelaram que ambos os materiais são superelásticos à temperatura ambiente e, portanto apresentaram composição basicamente austenítica de sua matriz. Os resultados de ensaio de tração são condizentes com a caracterização térmica e estrutural, pois os materiais apresentam recuperação total de forma após ciclos de carga e descarga em tração. Ambos os materiais são ricos em titânio, um deles apresenta camada de óxido superficial enquanto o outro apresenta acabamento superficial. Apesar das propriedades similares a amostra 1 apresentou média de 77 ciclos até a falha, enquanto a amostra 2 resistiu a 1827 ciclos..

Palavras-chave: Fadiga; Superelasticidade; Efeito memória de forma; Materiais funcionais.

COMPARATIVE ANALYSIS OF TWO DIFFERENT NITI WIRES' PROPERTIES AND FATIGUE LIFE

Abstract

The aim of the present study was to evaluate, by rotary bending fatigue tests, the fatigue resistance of two different NiTi alloys under strain-controlled testing condition at 25°C. Besides that, the mechanical, thermal and structural properties of the wires were characterized by DSC, XRD, SEM/EDX and tensile tests. The results revealed that both materials were superelastic at room temperature and therefore presented an austenitic matrix and full shape recovery in load/unloading tests in tension. One of the samples has an oxide covered surface whilst the other has passed through a step of surface finishing. Also, it was determined that both materials are Ti-rich. Despite the similar properties, sample 1 presented 77 cycles to failure, while sample 2 resisted 1827 cycles.

Keywords: Fatigue; Superelasticity, Shape memory effect; Functional materials.

[1] *Graduanda do curso de Engenharia Metalúrgica, UFMG, Belo Horizonte, Minas Gerais, Brasil.*
[2] *Graduando do curso de Engenharia Metalúrgica, UFMG, Belo Horizonte, Minas Gerais, Brasil.*
[3] *Engenheiro metalurgista, mestrando, PPGEM/UFMG, Belo Horizonte, Minas Gerais, Brasil.*
[4] *Engenheira metalurgista, doutoranda, PPGEM/UFMG, Belo Horizonte, Minas Gerais, Brasil.*
[5] *Engenheira de materiais, doutoranda, PPGEM/UFMG, Belo Horizonte, Minas Gerais, Brasil.*
[6] *Engenheiro de materiais, doutor, professor adjunto, DEMET/UFMG, Minas Gerais, Brasil.*
[7] *Físico, doutor, Professor titular, DEMET/UFMG, Minas Gerais, Brasil..*

1 INTRODUCTION

Near equiatomic NiTi alloys are widely used in applications in the medical and dental industries. It happens due to its high corrosion resistance and excellent biocompatibility, coupled with the functional properties of superelasticity and shape memory effect [1,2].

Superelasticity (SE) and shape memory effect (SME) are properties presented by materials capable of recovering strain levels that would be permanent for the most part of the alloys. NiTi can recover strains up to 8% in tension as a result of a reversible solid state phase transition. The martensitic transformation involves an austenitic (B2) high temperature matrix transforming into a low temperature martensitic (B19') phase by a shear mechanism in which atoms move short distances cooperatively. Phase instability is the driving force that promotes transformation. However, the transformation temperatures upon cooling, Ms and Mf, differs from the heating transformation temperatures, As and Af. This is what determines the hysteresis loop associated to a full cycle of loading/unloading or cooling/heating of NiTi alloy [3].

The SME is observed when the structure is deformed below its As temperature. As a result, an amount of martensite is stabilized producing a pseudo-plastic shape change that is recovered after a heating above Af. SE is a special case of SME in which the shape change occurs above Af, inducing the martensite formation by tension. In this case, the recovery occurs simply by the withdrawal of the load. The reverse transformation of martensite to austenite occurs, in both cases, to return to their initial forms [3].

Both in medical and dental use, NiTi alloys applications require resistance to repetitive stresses, since it is used as endodontic files, arterial stents and bone implants [4,5]. Thus, besides the concerns related to the biological response to its use, these applications involve the risk of fatigue failure, which occurs without previous macroscopic signs and may lead to unexpected complications [6,7].

Fatigue of materials refers to the changes in properties resulting from application of cyclic loads in strain or load control [8]. The fatigue behavior of NiTi alloys is not yet completely understood, mostly because of its non linear mechanical behavior [9]. Cyclic loads cause a big impact on the global response of NiTi alloys, due not only to the imposed structural damage, but also to the functional properties degradation related to the repeated phase transformation cycles [10].

The aim of the present study is to evaluate the fatigue resistance of two different Ni-Ti alloys under strain controlled testing condition at 25°C, and also to characterize its mechanical, thermal and structural properties.

2 DEVELOPMENT

2.1 Materials and methods

Two commercial NiTi wires, samples 1 and 2, with a nominal diameter of 1 mm were used in this study. At first, for comparative analysis, it is of essential importance to

determine their microstructural characteristics. The methods used for this purpose will be presented below.

2.1.1 Differential Scanning Calorimetry

Differential Scanning Calorimetry (DSC- DSC60 Shimadzu, Tokyo, Japan) analysis were made using three samples of approximately 5 mg each put into standard aluminum pans. Data were collected at a heating/cooling rate of 10°C/min over a temperature range of -100°C to 100°C. Transformation temperatures were determined with TA60-WS software, based on the tangent`s method.

2.1.2 X-Ray Diffraction

X-ray diffraction (XRD) was performed using a Panalytical PW1710 (Almelo, The Netherlands) with Bragg-Brentano geometry equipped with CuKα source (λ = 0,15418 nm) and scan rate of 0,02°/s. Measurements were taken in a range of 20° < 2θ < 120°. Phase identification was done comparing the obtained results with diffraction patterns available on the Inorganic Crystal Structure Database (ISCD).

2.1.3 Scanning Electron Microscopy

The wires were analyzed by secondary electron imaging (SEI) in a FEI S50 Inspect scanning electron microscope (SEM) to obtain qualitative information about the surface roughness and presence of oxide phases. In addition, samples were mounted in acrylic resin and its longitudinal section was exposed by grinding and polishing up to a mirror finishing. These sections were examined by backscattered electron (BSE) imaging to quantify the amount of second phases and by energy dispersive X-ray Spectroscopy (EDX) over ten areas to determine its semi-quantitative composition. Twelve micrographs were taken and analyzed with ImageJ software to determine the second phase fraction.

2.1.4 Tensile Test

Tensile tests were conducted at room temperature in an Instron 5582 universal testing machine with specimens cut in a total length of 120 mm, with 60 mm gauge length. Initially, the samples were strained up to 6% and unloaded, then loaded until rupture. Strain rates were chosen according to ASTM F2516-14 standard.

2.1.5 Rotary Bending Fatigue

To perform fatigue tests, a 27.2 mm section was bent into a 13 mm radius semi-circular shape, inducing a controlled strain level of 4%. Then, the specimen is forced to rotate along its axis by a motor attached to one end and the number of cycles to failure (Nf) was assessed by a inductive proximity sensor. The tests were carried in a temperature controlled water bath at 25°C and the rotational speed was set to approximately 52 rpm. Rotary bending fatigue tests were performed using a guided rotary bend tester as shown in Fig. 1.

2.1.6 Statistical analysis

The results were analyzed with the R language and environment for statistical computing [11]. To compare results of each group Welch two sample t-tests were performed, the assumption of normality of results was also checked. All conclusions were based on a significance level of 95% (α=0.05).

Figure 1; Rotary bending fatigue machine Analógica 8042.

2.2 Results

2.2.1 DSC

Both samples presented two transformation peaks, one upon cooling and one during heating. Samples 1 and 2 have their Af temperatures below room temperature (~25°C) indicating that when transformed to martensite they are prone to reverse the transformation towards an austenitic stable phase. Table 1 summarizes all the temperature transformation determined for the materials.

Table 1. Transformation temperatures determined by DSC. The results are presented as mean (SD) in °C

	As	Af	Ms	Mf
Sample 1 (A)	**-29.7 (1,3)**	**4.9 (0.6)**	**1.3 (0.5)**	**-23.7 (1.9)**
Sample 2 (B)	**-20.3 (3.7)**	**12.6 (0.8)**	**4.1 (2.3)**	**-19.0 (1.5)**

2.2.2 XRD

The samples have a characteristic phase composition of superelastic NiTi materials, their substrates are mainly austenitic. The diffraction pattern of sample 1, figure 1A, differs from sample 2 (1B) due to the presence of surface oxides. Also, the existence of Ni-rich compounds is noticed for sample 1.

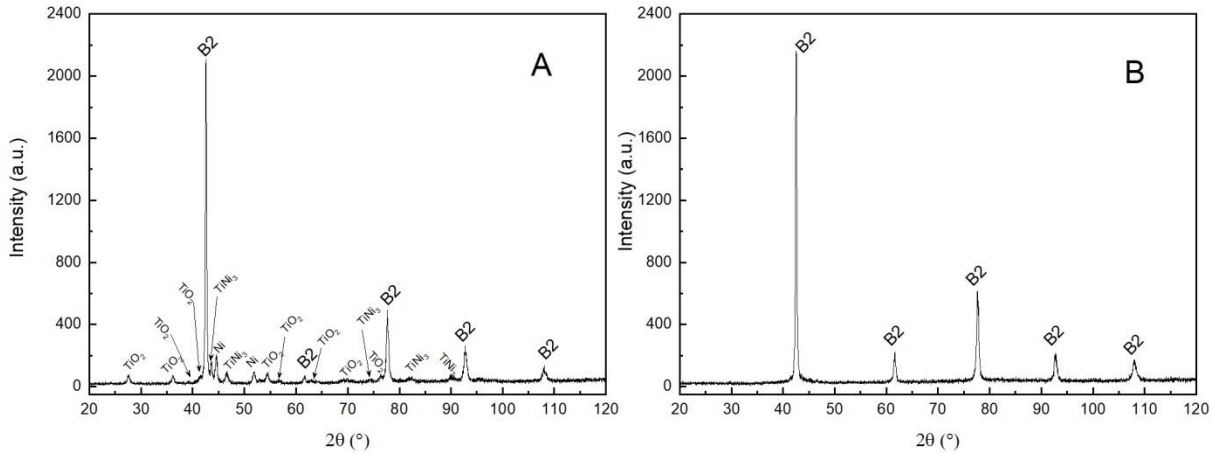

Figure 2. XRD patterns for (A) sample 1 and (B) sample 2.

2.2.3 SEM/EDX

The surface of the wires was observed at same operational conditions of the microscope. It can be seen in figure 2A that sample 1 has cracks and delamination over its surface oriented along its drawing axis. Figure 2B shows that the surface of sample 2 suffered some surface treatment that could eliminate the oxide layer producing a lower apparent surface roughness. In addition, some scratches can be seen suggesting mechanical surface finishing.

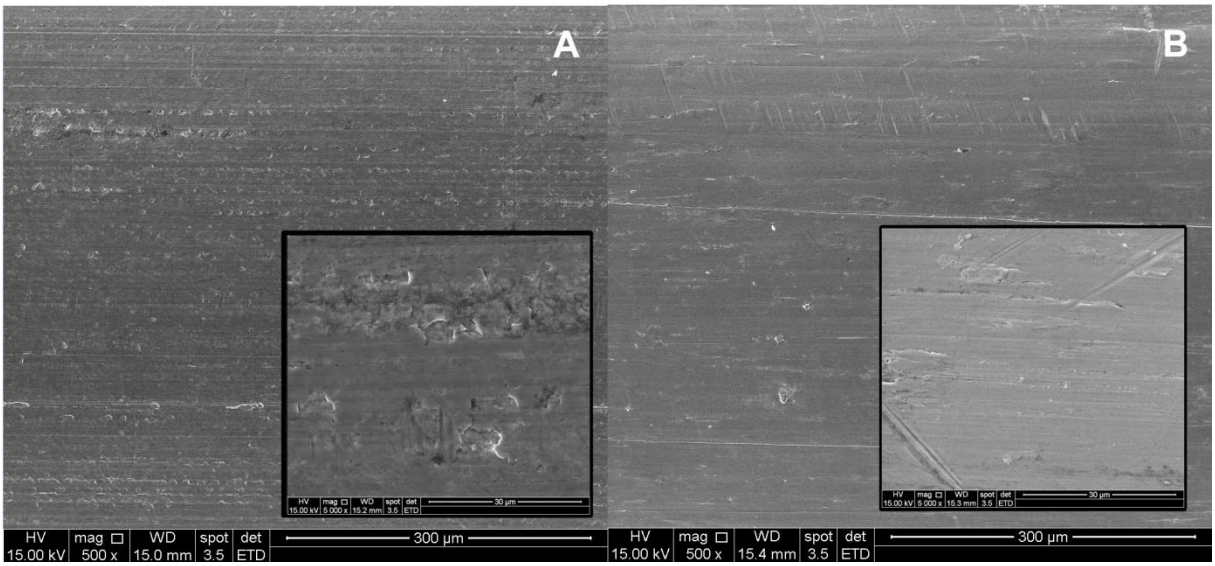

Figure 3. Electronic microscopy for (A) sample 1 and (B) sample 2. Insets show 5000x magnification of the pictures taken.

Sample 1 presented an atomic composition of 46.7% Ni and sample 2 has a composition of 49.8% Ni, both determined by EDX. The difference between the two results was significant.

Figure 4 shows the inclusions presented in the material and the elongated shapes suggest a relation with the treatment used during the samples' manufacturing process. The second phase seen on figure 4 also had its composition determined by EDX, the atomic nickel to titanium ratio of the precipitates is 1:2, leading to the conclusion that it consists of Ti_2Ni. The volume fraction of the second phase in each

sample was not different for both sample groups and its average value is equal to 0.6.

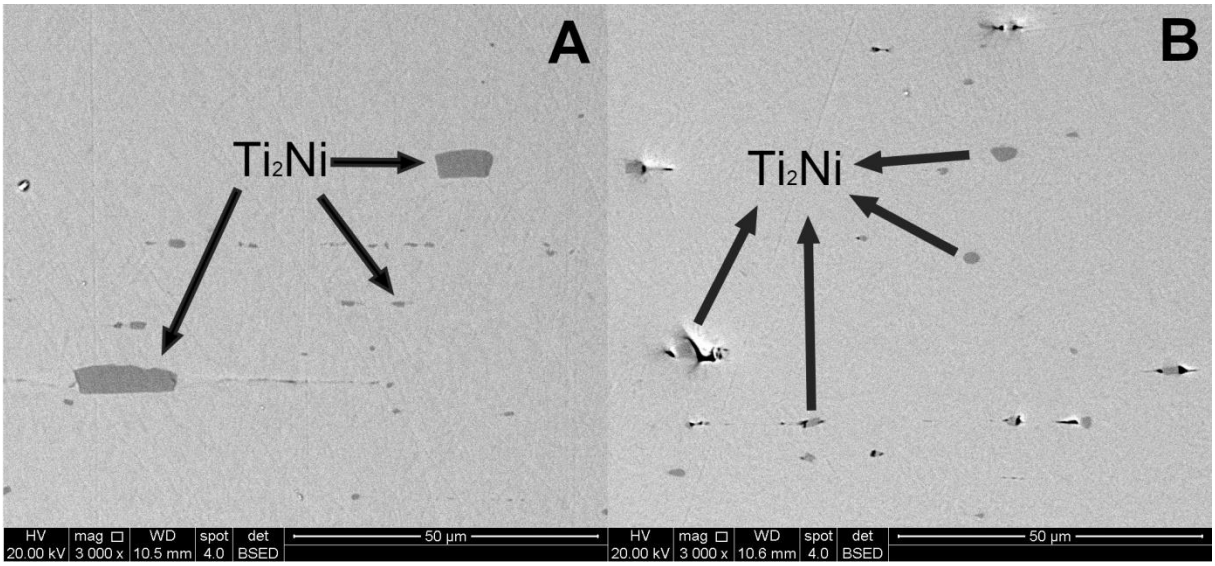

Figure 4. Electronic microscopy of the polished section for (A) sample 1 and (B) sample 2.

2.2.4 Tensile and fatigue tests

The uniaxial stress-strain properties in tension at 25ºC for both wires are shown in Fig 5. The curves have the characteristic shape of superelastic NiTi materials. It can be seen that the samples presented similar behavior at the same testing conditions. In the load/unload cycle sample 1 (5A) presents upper plateau stress (UPS) transformation of approximately 500 MPa, while sample 2 (5B) has UPS of approximately 450 MPa. The same trend can be noted for the lower plateau stress (LPS) transformation, sample 1 presenting values around 225 MPa and sample 2 with LPS around 175 MPa. Both samples have nearly equal total elongation and ultimate tensile strength, of 12% and 1200 MPa, respectively.

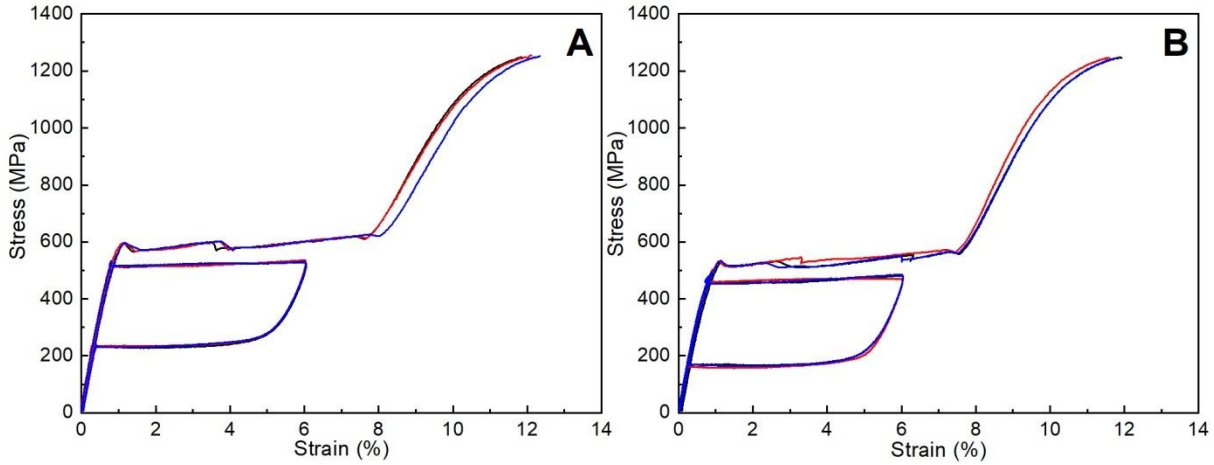

Figure 5. Tensile Tests for (A) sample 1 and (B) sample 2.

Sample 1 presented low fatigue resistance compared to sample 2, the first has an average fatigue life of 77 cycles against 1827 cycles of sample 2. Both average values presented an experimental error of 8% around the mean value and the mean values are significantly different.

2.3. DISCUSSION

Both samples presented consistent results regarding its phase composition, transformation temperatures and mechanical properties. Samples 1 and 2 have Af temperatures below 25°C, which means that any martensitic phase, whether transformed by stress or temperature change, tends to recover its original B2 structure and shape. This fact can be directly observed on the first cycle of load/unloading of the stress-strain curves as a complete shape recovery. It is important to highlight that the difference between the stress plateau on the first cycle and the plateau of the second loading is that in the test that went up to the fracture point the strain rate was ten times faster, as required by the followed standard for superelastic tension testing. It is also possible to notice that the difference between both samples remains at 50 MPa as in the first cycle. Also, the XRD results confirm that the substrate main phase is austenitic.

It can be seen in figure 2A that some other phases are present in the sample 1 material. They consist in TiO_2, Ni-rich compounds and even in pure Ni. These phases appear as a result of the material surface oxidation. Titanium oxidizes to TiO_2 preferentially due to thermodynamical reasons - TiO and NiO formation leads to lower free energy losses - thus these reactions are suppressed. When Ti in NiTi phase is oxidized at the surface a local Ni enrichment occurs at the subsurface of the material and depending on the diffusivity of the elements this Ni-rich layer can be thickened and form compounds and pure nickel phases. Heat treatments in furnaces with air environment are the typical situations that can lead to the referred situation, similar to sample 1. [12, 13]

The difference between the surfaces of each of the materials can be clearl observed in figure 3. Sample 1 has cracks and delaminated sections along its axis that can be related to thick oxide phases. The oxide formation leads to a density lowering given an amount of oxidized titanium, which means that 1 mol of Ti in solid solution is denser than the formed 1 mol of TiO_2. This incompatibility can lead to crack formation once the oxide grows on top of the denser material. Sample 2 has some evidences of mechanical surface finishing such as scratches along its axis (horizontal in all pictures) and apparent surface roughness diminishing.

The chemical composition of the alloys is rich in titanium, which leads to an interesting analysis of the results. NiTi phase is an intermetallic with certain solubility on the Ni-rich side of the phase diagram at sufficiently high temperatures. At the Ti-rich side the solubility is nearly zero as the boundary of NiTi and Ti_2Ni phases is almost vertical, which can be observed in figure 6. On the case of Ti-rich alloys the excess of titanium precipitates as Ti_2Ni and the matrix has a behavior similar to an equiatomic alloy.[2] The second phase fractions determined by image analysis show that a similar amount of phase is present in both materials. However, the expected amount of Ti_2Ni should be different given the fact that their chemical composition differ significantly, this may be related to an insufficient number of images taken into account to determine precipitated second phase fraction.

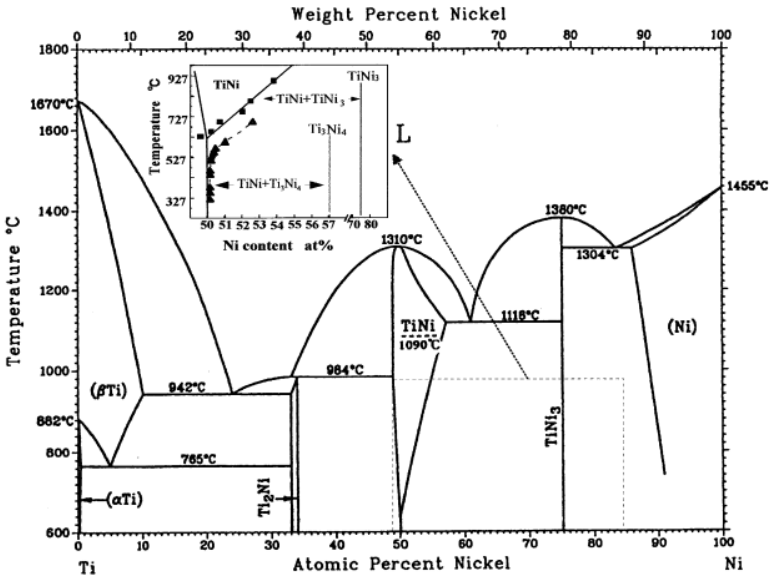

Figure 6. Ni-Ti phase diagram. The inset shows the metastable equilibrium of Ti3Ni4.[2]

The transformation temperatures of NiTi alloys depend on the chemical composition and on its thermomechanical history. Variation of Ms is neglectable below 50%at. Ni and tends to decay in compositions above equiatomic.[2] For Ni-rich alloys the easiest way to change the transformation temperatures of NiTi is ageing in order to induce precipitation of metastable Ti_3Ni_4 that hardens the parent phase and also changes the nickel content in the matrix, thus enhancing shape memory and pseudoelastic phenomena. Aging controlled temperature changes are not an option for an equiatomic matrix, and then the only mechanism available to do it is cold working.

In spite of all the similarities between both materials the fatigue resistance difference is quite large. Sample 1 mean fatigue life represents something about 4% of sample 2 mean fatigue life. None of all the measured properties varies in such manner.

The fatigue resistance of a given material depends on the imposed strain amplitude, strain variation frequency, environmental temperature, surface finishing, medium in which the material is subjected to load, its mechanical properties and others. Compared to other structural materials NiTi is capable to withstand high strain amplitudes and high number of cycles before failure. [6,9] In the present study all variables remained constant, in exception of the tested material. Martensitic transformation of NiTi plays an important role on its fatigue resistance, it is established that B19' is more resistant to fatigue failure than B2 phase. Also, as the strain increases at the point where stress induced transformation can be noticed an increase on the fatigue resistance occurs, this effect is also called Z-effect.[9] Martensitic transformation acts as an energy dissipator and slows the crack propagation that is also delayed by the ramification of the main crack in shorter small cracks, then extending the number of cycles to failure.[6]

In the present study it is difficult to come to a final answer to the question of what is the main cause to such fatigue resistance difference in materials that are quite similar. At first, sample 1 has a rougher surface finishing, characteristic that can lead to early crack initiation then earlier failure. Both samples present superelastic

behavior, however sample 1 has lower Af temperature and consequently higher martensite formation stress, then the activation of mechanisms that diminish crack propagation speed might be delayed compared to sample 2. Differences in transformation temperatures are not expected for two samples of equiatomic matrix if they do not differ in their amount of cold work. In sample 2 cross section it can be noticed that voids along the cold drawing axis around non deformable precipitates are present, suggesting that this sample has passed through a more intense cold work step. This evidence is in accordance to its higher transformation temperatures that arises from martensite stabilization upon cold deformation.

All the factors can be affecting the fatigue resistance of the materials together at the same time. Further investigation of its substructure properties might be the key to a complete understanding of this issue.

3 CONCLUSION

The conclusions that can be obtained from this work are listed below.

- Both materials presented Af temperatures below room temperature;
- Samples were constituted by an austenitic matrix. Sample 1 has an oxide surface provenient from the manufacturing process;
- Sample 1 has cracks on its oxide surface while sample 2 has a lower apparent roughness;
- Both samples have Ti_2Ni precipitates on the B2 matrix revealed by cross section microscopy;
- The samples presented superelasticity with full shape recovery after 6% load/unloading cycle;
- Despite all the similarities, sample 1 presented a considerably lower fatigue resistance compared to sample 2.

Acknowledgments

This work was partially supported by Coordenação de Aperfeiçoamento de Pessoal de Nível Superior (CAPES/PROEX) – Finance code 001, Brasília, DF, Brazil; Conselho Nacional de Desenvolvimento Científico e Tecnológico (CNPq), Brasília, DF,Brazil; Fundacão de Amparo à Pesquisa do Estado de Minas Gerais (FAPEMIG), Belo Horizonte, MG, Brazil; and Pro-Reitoria de Pesquisa da Universidade Federal de Minas Gerais (PRPq/UFMG), Belo Horizonte, MG, Brazil.

REFERENCES

1 Feninat, F. El; Laroche, G.; Fiset, M.; Mantovani, D. Shape Memory Materials for Biomedical Applications. Advanced Engineering Materials. 2002;4(3):91–104.

2 Otsuka, K.; Ren, X. Physical metallurgy of Ti – Ni-based shape memory alloys. Progress in Materials Scienc. 2005;50:511–678.

3 Otsuka, K.; Wayman, C. M. Shape Memory Materials. Cambridge ed. Cambridge University Press, 1998.

4 Gall, K.; Tyber, J.; Wilkesanders, G.; et al. Effect of microstructure on the fatigue of hot-rolled and cold-drawn niti shape memory alloys. Materials Science & Engineering. 2008;486:389–403.

5 Weaver, J. D.; Gutierrez, E. J. Comparing Rotary Bend Wire Fatigue Test Methods at Different Test Speeds. Journal of Materials Engineering and Performance. 2015;24(12):4966–4974.

6 Figueiredo, A. M.; Modenesi, P.; Buono, V. Low-cycle fatigue life of superelastic NiTi wires. International Journal of Fatigue. 2009;31(4):751–758.

7 Dieter, G. E. Mechanical Metallurgy. Nova York: mcgraw-Hill Book Company. 1961.

8 Eggeler, G.; Hornbogen, E.; Yawny, A.;Heckmann, A.;Wagner, M. Structural and functional fatigue of niti shape memory alloys. Materials Science and Engineering. 2004;378:24-33.

9 Figueiredo, A. M.; Gonzalez, B. M.; Buono, V.; Modenesi, P. Fatigue life curves of NiTi alloys – the z effect. Materials Science Forum. 2010;643:69-77.

10 Maletta, C.; Sgambitterra, E.; Furgiuele, F.;Casati, R.; Tuissi, A. Fatigue properties of a pseudoelastic NiTi alloy: Strain ratcheting and hystreresis under cyclic tensile loading. International Jounal of Fatigue. 2014;66:78-85.

11 R Core Team. R: A language and environment for statistical computing. Vienna, Austria. 2014. Disponível em: http://www.r-project.org/.

12 Mahmud, A.; Wu, Z.; Zhang, J.; Liu, Y.; Yang, H. Surface oxidation of NiTi and its effects on thermal and mechanical properties. Intermetallics. 2018;103:52:62.

13 Wu, Z.; Mahmud, A.; Zhang, J.; Liu, Y.; Yang, H. Surface oxidation of NiTi during thermal exposure in flowing argon environment. Materials and Design. 2018;140:123:133.